Zhao, Yanchong; Du, Luojun; Yang, Wei; Shen, Cheng; Tang, Jian; Li, Xiaomei; Chu, Yanbang; Tian, Jinpeng; Watanabe, Kenji; Taniguchi, Takashi; Yang, Rong; Shi, Dongxia; Sun, Zhipei; Zhang, Guangyu

# Observation of logarithmic Kohn anomaly in monolayer graphene

*Published in:*
Physical Review B

*DOI:*
10.1103/PhysRevB.102.165415

Published: 23/10/2020

*Document Version*
Publisher's PDF, also known as Version of record

*Please cite the original version:*
Zhao, Y., Du, L., Yang, W., Shen, C., Tang, J., Li, X., Chu, Y., Tian, J., Watanabe, K., Taniguchi, T., Yang, R., Shi, D., Sun, Z., & Zhang, G. (2020). Observation of logarithmic Kohn anomaly in monolayer graphene. *Physical Review B*, *102*(16), Article 165415. https://doi.org/10.1103/PhysRevB.102.165415

# Observation of logarithmic Kohn anomaly in monolayer graphene

Yanchong Zhao,[1,2] Luojun Du,[3,*] Wei Yang,[1,2,7] Cheng Shen,[1,2] Jian Tang,[1,2] Xiaomei Li,[1,2] Yanbang Chu,[1,2] Jinpeng Tian,[1,2] Kenji Watanabe,[4] Takashi Taniguchi,[5] Rong Yang,[1,6,7] Dongxia Shi,[1,2,6] Zhipei Sun,[3,8] and Guangyu Zhang[1,2,6,7,†]

[1]*Beijing National Laboratory for Condensed Matter Physics, Key Laboratory for Nanoscale Physics and Devices, Institute of Physics, Chinese Academy of Sciences, Beijing, 100190, China*
[2]*School of Physical Sciences, University of Chinese Academy of Science, Beijing 100190, China*
[3]*Department of Electronics and Nanoengineering, Aalto University, Tietotie 3, FI-02150, Finland*
[4]*Research Center for Functional Materials, National Institute for Materials Science, 1-1 Namiki, Tsukuba 305-0044, Japan*
[5]*International Center for Materials Nanoarchitectonics, National Institute for Materials Science, 1-1 Namiki, Tsukuba 305-0044, Japan*
[6]*Beijing Key Laboratory for Nanomaterials and Nanodevices, Beijing 100190, China*
[7]*Songshan-Lake Materials Laboratory, Dongguan, Guangdong Province 523808, China*
[8]*QTF Centre of Excellence, Department of Applied Physics, Aalto University, FI-00076 Aalto, Finland*

(Received 25 August 2020; revised 15 September 2020; accepted 17 September 2020; published 23 October 2020)

Electron-phonon coupling in monolayer graphene breaks the adiabatic Born-Oppenheimer approximation and could lead to exotic logarithmic Kohn anomaly, manifested as logarithmic singularity in optical-phonon energy. However, unraveling unambiguously the fascinating logarithmic Kohn anomaly in monolayer graphene remains challenging due to the large carrier inhomogeneity originating from the unique massless Dirac-like band dispersion and the underneath substrate doping effect. Here we demonstrate a clear signature of intriguing logarithmic Kohn anomaly in monolayer graphene with ultralow carrier inhomogeneity via *h*-BN encapsulation. Significantly, the magnitude of anomalous phonon softening at 25 K shows an enhancement factor of 2 as compared to that previously observed in bilayer graphene at 12 K, even though bilayer graphene with nearly parabolic band dispersion is more immune to charged impurities. The uncovered unusual logarithmic Kohn anomaly in monolayer graphene can provide a firm basis for the understanding of various peculiar physics and may shed light on the nature of superconductivity in magic-angle graphene superlattices.

DOI: 10.1103/PhysRevB.102.165415

## I. INTRODUCTION

Electron-phonon interactions (EPIs), also referred to as electron-phonon coupling, are the cornerstone of many-particle physics and underpin a rich variety of fascinating physical phenomena [1–5], including but not limited to superconductivity [6,7], charge-density wave [8,9], intervalley scattering [10,11], linear-in-temperature resistivity [12–14], and ultrafast carrier dynamics [15–17]. Usually, EPIs are described within the scope of adiabatic Born-Oppenheimer (ABO) approximation. In contrast, when the phonon frequency or electron-phonon coupling strength is comparable to the electron Fermi energy, unconventional EPIs beyond ABO approximation can occur [18,19]. The breakdown of ABO approximation may enable a wide variety of exciting physical behaviors, such as nonadiabatic superconducting pairing with high $T_c$ [20,21], electronic correlation effects [7,22], and the giant renormalization of phonon dispersion relations and electronic properties [23–29].

Monolayer graphene with unique massless Dirac-like band dispersion and strong electron-phonon coupling strength provides an unprecedented arena to realize tunable EPIs beyond ABO approximation under the two-dimensional limit [30,31]. Recent studies based on second-order time-dependent perturbation theory point out that the EPIs in monolayer graphene are nonadiabatic and beyond ABO approximation, resulting in the giant energy renormalization for long-wavelength $E_{2g}$ phonon at the Brillouin zone center (Raman $G$ peak) and fascinating logarithmic Kohn anomaly (LKA) [32–35]. Specifically, the self-energy ($\Pi$) of the $G$ band Green's function under Fermi energy ($E_F$) is [32,33]

$$\Pi = \alpha|E_F| - \frac{1}{4}\alpha(\hbar\omega_0 + i\zeta)\left[\ln\left|\frac{\hbar\omega_0 + |2E_F| + i\zeta}{\hbar\omega_0 - |2E_F| + i\zeta}\right| + \pi i\right], \tag{1}$$

where $\alpha$ is the electron-phonon coupling parameter with dimensions of energy ($4.43 \times 10^{-3}$), $\hbar\omega_0$ denotes the energy of the $G$ band ($\sim$196 meV), and $\zeta$ is the level broadening effect originating from carrier inhomogeneity or temperature effect. Figure 1(a) presents the evolution of phonon frequency shift (real part of $\Pi$), defined as $\hbar\omega(E_F) - \hbar\omega_0$, as a function of Fermi energy at different $\zeta$. Please refer to the Supplemental Material [36] for the $E_F$-dependent phonon lifetime (imaginary part of $\Pi$). For $\zeta = 0$, the phonon energy of monolayer graphene diverges logarithmically to $-\infty$ when $|E_F| = \frac{\hbar\omega_0}{2}$,

*luojun.du@aalto.fi
†gyzhang@iphy.ac.cn

 

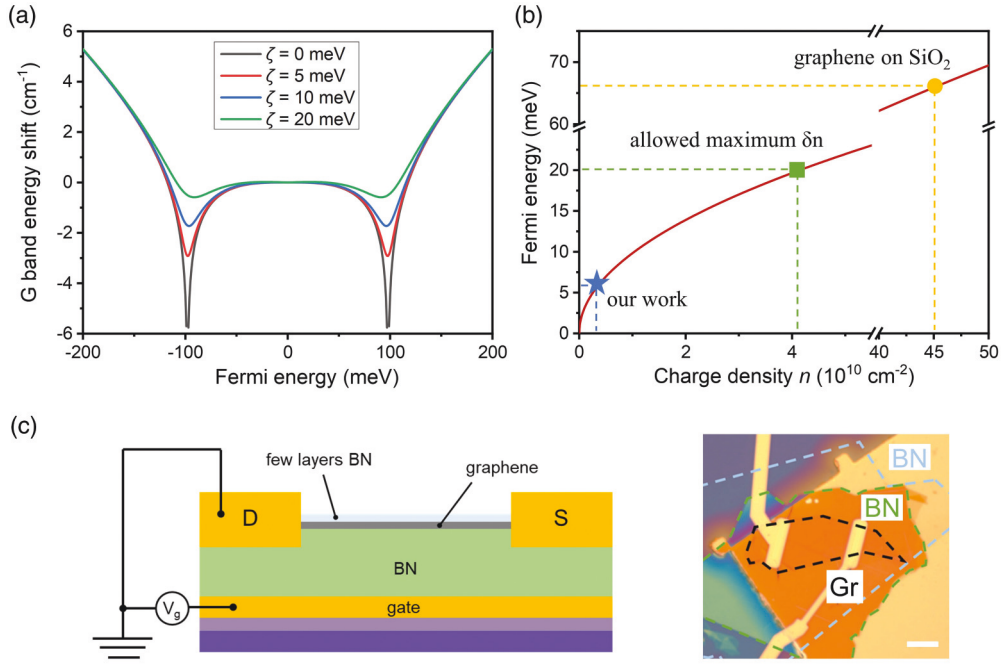


FIG. 1. Logarithmic Kohn anomaly in monolayer graphene. (a) $G$ band frequency shift as a function of Fermi energy at different $\zeta$, calculated by the real part of self-energy $\Pi$. (b) Fermi energy versus the carrier density. Blue star (yellow circle) represents the carrier inhomogeneity ($\delta n$) in our device (monolayer graphene on $SiO_2$/Si substrate), and the green square represents the allowed maximum $\delta n$ for observation of LKA in theory. (c) Schematic structure (left) and white-light microscope image (right) of the $h$-BN encapsulated monolayer graphene FET with one-dimensional electrical contact. The locations of monolayer graphene, top $h$-BN, and back $h$-BN are outlined with the black, blue, and green dashed line, respectively. In order to achieve a good optical transparency, the thickness of top $h$-BN is less than 4 nm. Scale bar, 10 $\mu$m.

known as the exotic LKA [32,33]. However, $\zeta$ cannot be zero in real situations and LKA would be gradually washed out by increasing $\zeta$. In order to see LKA clearly, $\zeta$ should be ideally less than 20 meV [Fig. 1(a)]. In the light of the peculiar Dirac linear energy-momentum dispersion of monolayer graphene [$E_F = -\mathrm{sgn}(n)\beta\sqrt{\pi|n|}$, where $n$ indicates carrier density, $E_\mathrm{F}$ denotes the Fermi energy, sgn($x$) is the sign of $x$, and $\beta = 5.52\,\mathrm{eV\,\AA}$ is the slope of electron bands], the allowed maximum charge inhomogeneity $\delta n$ for the observation of LKA cannot exceed $\sim 4.15 \times 10^{10}\,\mathrm{cm}^{-2}$ [Fig. 1(b)]. For monolayer graphene on $SiO_2$ substrate previously studied [37–44], the typical carrier density fluctuation is usually up to the order of $10^{11}\,\mathrm{cm}^{-2}$ [45–47]. As a result, the intriguing LKA still remains elusive in monolayer graphene even more than 10 years after the theoretical prediction [32,33].

Here we fabricate the high-quality monolayer graphene field effect transistor (FET) with ultralow carrier inhomogeneity (e.g., $\sim 3.3 \times 10^9\,\mathrm{cm}^{-2}$) by encapsulating with thin layers of hexagonal boron nitride ($h$-BN). Through measuring the evolution of Raman spectra as a function of $E_\mathrm{F}$, we uncover the significant phonon softening at $|E_\mathrm{F}| = \frac{\hbar\omega_0}{2}$ and demonstrate the clear evidence of exotic LKA in monolayer graphene. The observation of LKA in monolayer graphene would provide a firm basis for various unique phenomena. In addition, considering that the nonadiabatic EPIs may play a vital role in the superconducting pairing of twisted bilayer graphene [13,14,48–55], our work might spark significant attention and may offer insight into the underlying physics of superconductivity in magic-angle graphene superlattices.

## II. RESULTS

As shown in previous studies, charge inhomogeneity in monolayer graphene can be significantly reduced by applying $h$-BN encapsulation [56]. To realize ultralow carrier inhomogeneity, we prepare $h$-BN encapsulated monolayer graphene by a van der Waals mediated dry transfer approach employing the propylene carbonate (PC) stamp, as outlined in Figs. S2(a)–S2(d) in the Supplemental Material [36,57–59]. The atomically smooth surfaces of $h$-BN are free of dangling bonds and can strongly reduce the formation of electron-hole puddles [56,60]. Briefly, monolayer graphene and thin $h$-BN flakes are first exfoliated onto silicon substrates with a 280-nm-thick oxide layer. PC stamps are used to pick up a thin $h$-BN flake, monolayer graphene and another $h$-BN flake in sequence with accurate alignment based on an optical microscope. The sandwiched $h$-BN/monolayer graphene/$h$-BN heterostructures are then transferred onto a $SiO_2$/Si substrate with a prepatterned Ti/Au electrode as the back gate. Compared to normal devices with degenerately doped silicon as the back gate, the local Ti/Au back gate used here can effectively screen the charged impurities on $SiO_2$ substrates and thus reduce the carrier inhomogeneity. Finally, electron-beam lithography, reactive ion etching, and electron-beam evaporation are used to obtain the one-dimensional electrical contact with monolayer graphene [57]. Figure 1(c) shows the schematic diagram of the $h$-BN encapsulated monolayer graphene device, and the corresponding optical microscope image reveals the ultraclean interfaces. Note that, to rule out

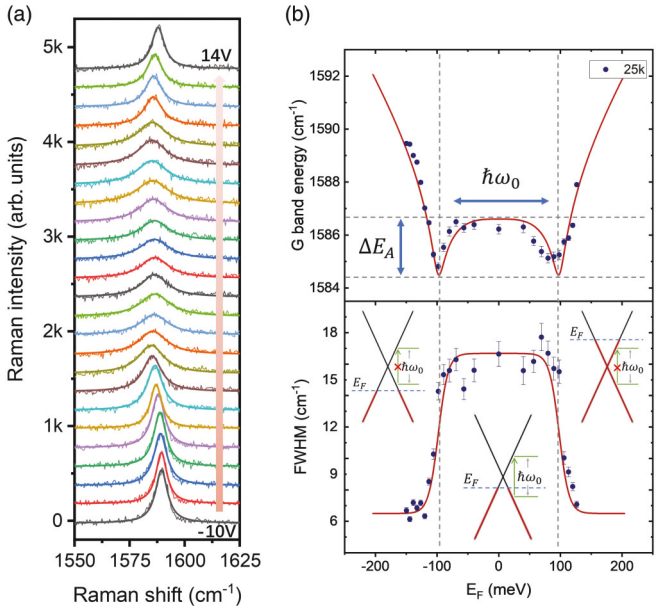


FIG. 2. Fermi energy dependent Raman $G$ mode at 25 K. (a) Raman spectra measured under different back-gate voltages. (b) $G$ band energy (upper panel) and linewidth (lower panel) as a function of Fermi energy. Inset: Landau damping of $G$ phonon into electron-hole pairs is only allowed when $|E_F| < \frac{\hbar\omega_0}{2}$ and is forbidden by the Pauli principle when $|E_F| > \frac{\hbar\omega_0}{2}$. Blue dots: measurements; red lines: theoretical calculation from Eq. (1) with $\zeta = 7.9$ meV.

the effect of moiré superlattices [61–65], the interlayer twist angle between monolayer graphene and $h$-BN flake is purposely controlled to deviate from 0° or 60°.

Based on the as-fabricated $h$-BN encapsulated monolayer graphene devices, we then measure the evolution of unpolarized Raman spectra against $E_F$ (back-gate voltage $V_{bg}$) to demystify the exotic LKA under the monolayer limit with confocal backscattering configuration in vacuum, excited by 532 nm (2.33 eV) laser radiation. The scattered signal is collected by an Olympus 50× long working distance objective and dispersed by a 1800 g mm$^{-1}$ grating to achieve Raman spectral resolution better than 1 cm$^{-1}$. To avoid laser-induced heating and photoinduced doping from defect transitions of $h$-BN flake [66], a relatively small incident power of ∼100 $\mu$W is used (see details in Supplemental Material [36]). Figure 2(a) displays the evolution of the Raman $G$ peak as a function of $V_{bg}$ at 25 K. Remarkably, both the phonon frequency and lifetime are strongly dependent on the $V_{bg}$. Through Lorentzian fitting, we determine the phonon energy and full width at half maximum (FWHM) at different $V_{bg}$. For a better comparison with the theoretical results of Eq. (1), we convert the $V_{bg}$ to $E_F$ using $E_F = -\mathrm{sgn}(n)\beta\sqrt{\pi|n|}$, where carrier density $n$ is defined as $n = \frac{C_{bg}(V_{bg}-V_{Dirac})}{e}$, with $e$ the elementary charge, $C_{bg}$ back-gate capacitance, and $V_{Dirac}$ the gate voltage corresponding to the charge-neutral Dirac point. The upper panel of Fig. 2(b) presents the extracted $G$ band energy (blue dots) as a function of $E_F$. With increasing $|E_F|$, the Raman $G$ mode first softens and then stiffens. In marked contrast to prior studies that phonon frequency monotonically stiffens with $|E_F|$ [37–41], here we uncover the phonon softening. Moreover, two anomalous minima are clearly observed at $E_F = \pm\frac{\hbar\omega_0}{2}$, revealing unambiguously the long-sought LKA in monolayer graphene. Significantly, the magnitude of anomalous phonon softening $\Delta E_A = \hbar\omega_0(E_F = 0) - \hbar\omega(E_F = \frac{\hbar\omega_0}{2})$ is about 2.1 cm$^{-1}$ at 25 K. This shows an enhancement factor of 2 as compared to the $\Delta E_A$ previously measured in bilayer graphene at a lower temperature of 12 K, even considering that bilayer graphene is a more robust case with nearly parabolic band dispersion and large density of states near the charge-neutral Dirac point [27,31].

Furthermore, our $E_F$-dependent $G$ band energy can be well fitted by the real part of Eq. (1) with $\zeta = 7.9$ meV [red line in upper panel of Fig. 2(b)], confirming that the two anomalous minima at $E_F = \pm\frac{\hbar\omega_0}{2}$ are indeed the manifestation of LKA. Considering that the Raman spectra are measured at 25 K, rather than absolute zero temperature, the thermal energy can definitely lead to the level broadening effect ($k_BT$) and thus contribute to $\zeta$. Deducting the temperature effect, $\zeta$ induced by carrier density fluctuations is about 5.7 meV, corresponding to the charge inhomogeneity $\delta n = 3.3 \times 10^9$ cm$^{-2}$ [Fig. 1(b)]. This is more than 100 times smaller than that for monolayer graphene on a $SiO_2$/Si substrate and 10 times smaller than the maximum $\delta n$ for the observation of LKA [45,47]. Benefiting from the ultralow carrier inhomogeneity, we can observe clearly the LKA and a large anomalous phonon softening in monolayer graphene. Note that the ultralow charge fluctuations obtained here are in good harmony with previous measurements by scanning tunneling spectroscopy ($\delta n = 2.5 \times 10^9$ cm$^{-2}$) [60], also suggesting that Raman scattering can act as an effective and simple optical method to determine the charge inhomogeneity.

The ultralow carrier inhomogeneity in our $h$-BN encapsulated monolayer graphene is further analyzed by the lifetime of the $G$ peak [lower panel of Fig. 2(b)]. The $E_F$-driven evolution of FWHM at 25 K (blue dots) shows an almost sudden change near $E_F = \pm\frac{\hbar\omega_0}{2}$ and can be well described by the imaginary part of $\Pi$ with $\zeta = 7.9$ meV (red line), which is the same as that used to fit the $G$ band energy with the real part of $\Pi$. Usually, the FWHM of a phonon can be written as $\gamma = \gamma^{\mathrm{ph-ph}} + \gamma^{e-\mathrm{ph}}$, where $\gamma^{\mathrm{ph-ph}}$ and $\gamma^{e-ph}$ are originated from the anharmonic phonon-phonon coupling and EPIs, respectively. When $|E_F| < \frac{\hbar\omega_0}{2}$, the $G$ phonon can decay into vertical electron-hole pairs [inset of lower panel in Fig. 2(b)], giving rise to the contribution $\gamma^{e-ph}$. In stark contrast, the Landau damping of the $G$ phonon is halted by the Pauli exclusion principle when $|E_F| > \frac{\hbar\omega_0}{2}$ [3,27,31,37,38]. As a consequence, the contribution of $\gamma^{e-ph}$ disappears, leading to the long-lived $G$ phonon and sudden reduction of FWHM. The total change in FWHM $[\gamma(E_F = 0) - \gamma(E_F = \infty)]$ is the magnitude of $\gamma^{e-ph}$. Importantly, calculations based on Fermi's "golden rule" show that the electron-phonon coupling strength $\langle D_\Gamma^2\rangle^2$ can be directly obtained from $\gamma^{(e-ph)}$: $\gamma^{(e-ph)} = \frac{\sqrt{3}a_0^2\hbar^2}{4M\beta^2}\langle D_\Gamma^2\rangle^2$, where $a_0$ and $M$ are the lattice spacing and the carbon atomic mass, respectively [3]. The measured $\gamma^{e-ph}$ in our $h$-BN encapsulated monolayer graphene is 10.3 cm$^{-1}$ $[\gamma(E_F = 0) - \gamma(E_F = 200\,\mathrm{meV})]$, corresponding to $\langle D_\Gamma^2\rangle^2 = 42.1$ (eV/Å)$^2$. This is in good agreement with the first-principles calculations $\langle D_\Gamma^2\rangle^2 = 45.6$ (eV/Å)$^2$ [3,30].

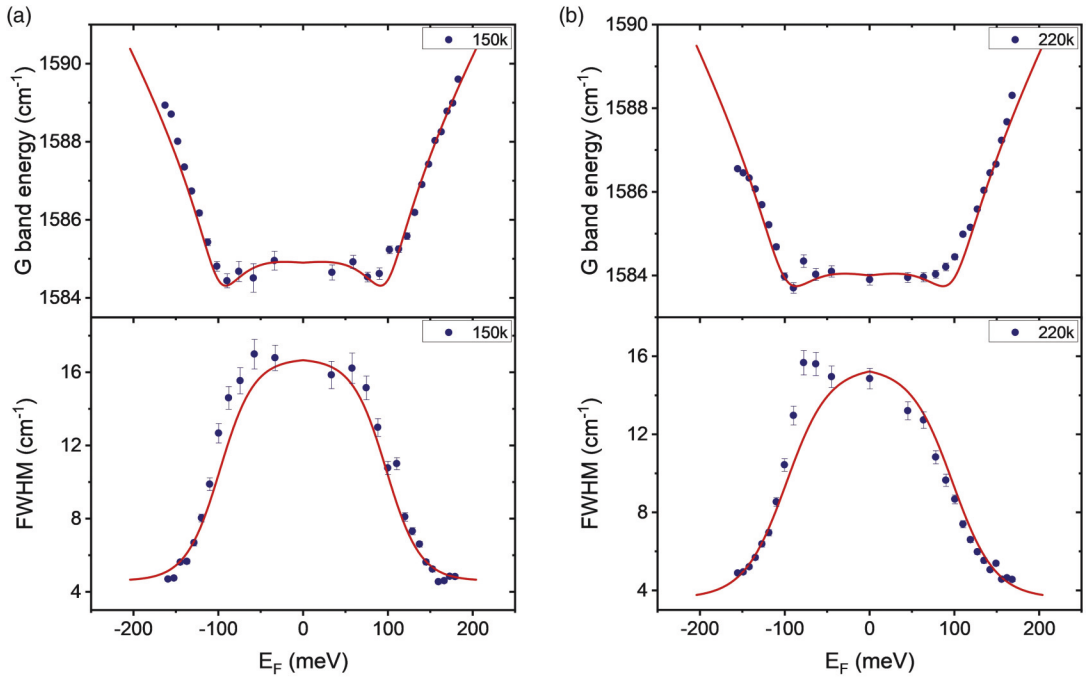


FIG. 3. $E_F$-driven evolution of Raman $G$ band at 150 K (a) and 220 K (b). Upper panel: $G$ band energy versus Fermi energy. Lower panel: the FWHM of the $G$ peak as a function of Fermi energy. Blue dots: measurements; red lines: theoretical calculation from Eq. (1) with $\zeta = 19.3$ meV (a) and 24.9 meV (b).

We would like to mention that the electron-phonon coupling strength in monolayer graphene is very large and can be comparable to that in well-known nonadiabatic high-$T_c$ superconductor $MgB_2$ [20,30,67]. Such giant electron-phonon coupling may also play a nontrivial role in the formation of nonadiabatic superconducting pairing in twisted bilayer graphene [21,49,53].

Finally, we measure the Raman spectra of $h$-BN encapsulated monolayer graphene at relatively high temperatures. Figures 3(a) and 3(b) show the $E_F$-dependent $G$ band energy (upper panel) and FWHM (lower panel) extracted via Lorentzian fit at 150 and 220 K, respectively. The experimental data (blue dots in Fig. 3) at 150 K (220 K) can be well fitted by Eq. (1) (red lines in Fig. 3) with $\zeta = 19.3$ meV (24.9 meV). Interestingly, two anomalous minima can still be distinguished at $E_F = \pm\frac{\hbar\omega_0}{2}$, clearly demonstrating the LKA. On the other hand, due to the temperature-induced level broadening effect, the magnitude of anomalous phonon softening $\Delta E_A$ at 150 K (220 K), as compared with that at 25 K, is largely reduced to only $\sim$0.6 cm$^{-1}$ ($\sim$ 0.3 cm$^{-1}$). In addition, the obtained $\zeta$ at 150 K (19.3 meV) and 220 K (24.9 meV) indicating that $\zeta$ originated from carrier density fluctuation is about 6.3 and 5.9 meV, respectively, being consistent with the value extracted at 25 K.

## III. CONCLUSION

We fabricate the high-quality $h$-BN encapsulated monolayer graphene device through a van der Waals mediated pickup, dry transfer method. Benefiting from the ultralow carrier inhomogeneity ($\sim 3.3 \times 10^9$ cm$^{-2}$), we uncover the significant anomalous phonon softening at $E_F = \pm\frac{\hbar\omega_0}{2}$ and thus demystify the fascinating LKA in monolayer graphene. The observation of LKA beyond ABO approximation, together with the giant electron-phonon coupling, would set a firm basis for various intriguing phenomena in monolayer graphene and may provide insight into the nature of the nonadiabatic superconducting pairing in twisted bilayer graphene.

## ACKNOWLEDGMENTS

G.Z. thanks the National Science Foundation of China (NSFC) under Grants No. 61888102 and No. 11834017, the Strategic Priority Research Program of Chinese Academy of Sciences (CAS) under Grant No. XDB0000000, the Key Research Program of Frontier Sciences of CAS under Grant No. QYZDB-SSW-SLH004, and the National Key R&D Program under Grant No. 2016YFA0300904. Z.S. gratefully acknowledges the financial support by the Academy of Finland (Grants No. 295777, No. 312297, and No. 314810), the Academy of Finland Flagship Programme (Grant No. 320167, PREIN), the European Union's Horizon 2020 Research and Innovation Program (Grant No. 820423, S2QUIP), and ERC (Grant No. 834742). W.Y. gratefully acknowledges the Strategic Priority Research Program of the Chinese Academy of Sciences (CAS) under Grant No. XDB33000000. L.D. gratefully acknowledges the financial support by the Academy of Finland (Grant No. 13333099). K.W. and T.T. acknowledge support from the Elemental Strategy Initiative conducted by the MEXT, Japan, Grant No. JPMXP0112101001, JSPS KAKENHI Grant No. JP20H00354, and the CREST (JPMJCR15F3), JST.

G.Z. supervised this work. L.D. proposed the project. Y.Z. and L.D. conceived and designed the experiments. Y.Z. fab-

ricated the devices, and performed the Raman measurements with technical assistance from L.D. Y.Z. and L.D. performed data analysis. K.W. and T.T. contributed high-quality *h*-BN crystals. Y.Z. and L.D. wrote the paper with comments from Z.S. and G.Z. All the other authors were involved in the discussion.


[1] F. Giustino, Rev. Mod. Phys. **89**, 015003 (2017).
[2] T. P. Devereaux and R. Hackl, Rev. Mod. Phys. **79**, 175 (2007).
[3] M. Lazzeri, S. Piscanec, F. Mauri, A. C. Ferrari, and J. Robertson, Phys. Rev. B **73**, 155426 (2006).
[4] L. Du, M. Liao, J. Tang, Q. Zhang, H. Yu, R. Yang, K. Watanabe, T. Taniguchi, D. Shi, Q. Zhang, and G. Zhang, Phys. Rev. B **97**, 235145 (2018).
[5] G. D. Mahan, *Many-Particle Physics* (Springer Science & Business Media, Berlin, 2013).
[6] J. Bardeen, L. N. Cooper, and J. R. Schrieffer, Phys. Rev. **108**, 1175 (1957).
[7] S. Gerber, S.-L. Yang, D. Zhu, H. Soifer, J. A. Sobota, S. Rebec, J. J. Lee, T. Jia, B. Moritz, C. Jia, A. Gauthier, Y. Li, D. Leuenberger, Y. Zhang, L. Chaix, W. Li, H. Jang, J.-S. Lee, M. Yi, G. L. Dakovski *et al.*, Science **357**, 71 (2017).
[8] M. Calandra, I. I. Mazin, and F. Mauri, Phys. Rev. B **80**, 241108(R) (2009).
[9] X. Xi, L. Zhao, Z. Wang, H. Berger, L. Forró, J. Shan, and K. F. Mak, Nat. Nanotechnol. **10**, 765 (2015).
[10] B. R. Carvalho, Y. Wang, S. Mignuzzi, D. Roy, M. Terrones, C. Fantini, V. H. Crespi, L. M. Malard, and M. A. Pimenta, Nat. Commun. **8**, 14670 (2017).
[11] J. Kim, C. Jin, B. Chen, H. Cai, T. Zhao, P. Lee, S. Kahn, K. Watanabe, T. Taniguchi, and S. Tongay, Sci. Adv. **3**, e1700518 (2017).
[12] D. K. Efetov and P. Kim, Phys. Rev. Lett. **105**, 256805 (2010).
[13] H. Polshyn, M. Yankowitz, S. Chen, Y. Zhang, K. Watanabe, T. Taniguchi, C. R. Dean, and A. F. Young, Nat. Phys. **15**, 1011 (2019).
[14] F. Wu, E. Hwang, and S. D. Sarma, Phys. Rev. B **99**, 165112 (2019).
[15] C. Jin, E. Y. Ma, O. Karni, E. C. Regan, F. Wang, and T. F. Heinz, Nat. Nanotechnol. **13**, 994 (2018).
[16] Y. Wang, Z. Wang, W. Yao, G.-B. Liu, and H. Yu, Phys. Rev. B **95**, 115429 (2017).
[17] F. Rossi and T. Kuhn, Rev. Mod. Phys. **74**, 895 (2002).
[18] E. Cappelluti and L. Pietronero, J. Phys. Chem. Solids **67**, 1941 (2006).
[19] L. Boeri, E. Cappelluti, and L. Pietronero, Phys. Rev. B **71**, 012501 (2005).
[20] E. Cappelluti, S. Ciuchi, C. Grimaldi, L. Pietronero, and S. Strässler, Phys. Rev. Lett. **88**, 117003 (2002).
[21] L. P. Gor'kov, Proc. Nat. Acad. Sci. USA **113**, 4646 (2016).
[22] Z. P. Yin, A. Kutepov, and G. Kotliar, Phys. Rev. X **3**, 021011 (2013).
[23] F. Caruso, M. Hoesch, P. Achatz, J. Serrano, M. Krisch, E. Bustarret, and F. Giustino, Phys. Rev. Lett. **119**, 017001 (2017).
[24] J. Tsang, M. Freitag, V. Perebeinos, J. Liu, and P. Avouris, Nat. Nanotechnol. **2**, 725 (2007).
[25] H. Farhat, H. Son, G. G. Samsonidze, S. Reich, M. S. Dresselhaus, and J. Kong, Phys. Rev. Lett. **99**, 145506 (2007).
[26] A. Das, B. Chakraborty, S. Piscanec, S. Pisana, A. K. Sood, and A. C. Ferrari, Phys. Rev. B **79**, 155417 (2009).
[27] J. Yan, E. A. Henriksen, P. Kim, and A. Pinczuk, Phys. Rev. Lett. **101**, 136804 (2008).
[28] L. M. Malard, D. C. Elias, E. S. Alves, and M. A. Pimenta, Phys. Rev. Lett. **101**, 257401 (2008).
[29] A. Lanzara, P. Bogdanov, X. Zhou, S. Kellar, D. Feng, E. Lu, T. Yoshida, H. Eisaki, A. Fujimori, and K. Kishio, Nature **412**, 510 (2001).
[30] S. Piscanec, M. Lazzeri, F. Mauri, A. C. Ferrari, and J. Robertson, Phys. Rev. Lett. **93**, 185503 (2004).
[31] A. C. Neto, F. Guinea, N. M. Peres, K. S. Novoselov, and A. K. Geim, Rev. Mod. Phys. **81**, 109 (2009).
[32] T. Ando, J. Phys. Soc. Jpn. **75**, 124701 (2006).
[33] M. Lazzeri and F. Mauri, Phys. Rev. Lett. **97**, 266407 (2006).
[34] A. H. Castro Neto and F. Guinea, Phys. Rev. B **75**, 045404 (2007).
[35] A. C. Ferrari and D. M. Basko, Nat. Nanotechnol. **8**, 235 (2013).
[36] See Supplemental Material at http://link.aps.org/supplemental/10.1103/PhysRevB.102.165415 for details on photon lifetime, sample fabrication, Raman spectra under different power and integral time, the evolution of G peak at room temperature.
[37] J. Yan, Y. Zhang, P. Kim, and A. Pinczuk, Phys. Rev. Lett. **98**, 166802 (2007).
[38] S. Pisana, M. Lazzeri, C. Casiraghi, K. S. Novoselov, A. K. Geim, A. C. Ferrari, and F. Mauri, Nat. Mater. **6**, 198 (2007).
[39] A. Das, S. Pisana, B. Chakraborty, S. Piscanec, S. K. Saha, U. V. Waghmare, K. S. Novoselov, H. R. Krishnamurthy, A. K. Geim, and A. C. Ferrari, Nat. Nanotechnol. **3**, 210 (2008).
[40] C. Stampfer, F. Molitor, D. Graf, K. Ensslin, A. Jungen, C. Hierold, and L. Wirtz, Appl. Phys. Lett. **91**, 241907 (2007).
[41] J. Yan, Y. Zhang, S. Goler, P. Kim, and A. Pinczuk, Solid State Commun. **143**, 39 (2007).
[42] A. C. Ferrari, Solid State Commun. **143**, 47 (2007).
[43] L. Malard, M. Pimenta, G. Dresselhaus, and M. Dresselhaus, Phys. Rep. **473**, 51 (2009).
[44] G. Froehlicher and S. Berciaud, Phys. Rev. B **91**, 205413 (2015).
[45] J. Martin, N. Akerman, G. Ulbricht, T. Lohmann, J. H. Smet, K. von Klitzing, and A. Yacoby, Nat. Phys. **4**, 144 (2008).
[46] K. I. Bolotin, K. J. Sikes, Z. Jiang, M. Klima, G. Fudenberg, J. Hone, P. Kim, and H. Stormer, Solid State Commun. **146**, 351 (2008).
[47] Y. Zhang, V. W. Brar, C. Girit, A. Zettl, and M. F. Crommie, Nat. Phys. **5**, 722 (2009).
[48] D. Szczęśniak and R. Szczłśniak, Phys. Rev. B **99**, 224512 (2019).
[49] B. Lian, Z. Wang, and B. A. Bernevig, Phys. Rev. Lett. **122**, 257002 (2019).
[50] Y. W. Choi and H. J. Choi, Phys. Rev. B **98**, 241412(R) (2018).
[51] M. Koshino and N. N. T. Nam, Phys. Rev. B **101**, 195425 (2020).
[52] S. D. Sarma and F. Wu, Ann. Phys. **417**, 168193 (2020).

[53] F. Wu, A. H. MacDonald, and I. Martin, Phys. Rev. Lett. **121**, 257001 (2018).
[54] T. J. Peltonen, R. Ojajärvi, and T. T. Heikkilä, Phys. Rev. B **98**, 220504(R) (2018).
[55] I. Yudhistira, N. Chakraborty, G. Sharma, D. Y. H. Ho, E. Laksono, O. P. Sushkov, G. Vignale, and S. Adam, Phys. Rev. B **99**, 140302(R) (2019).
[56] C. R. Dean, A. F. Young, I. Meric, C. Lee, L. Wang, S. Sorgenfrei, K. Watanabe, T. Taniguchi, P. Kim, and K. L. Shepard, Nat. Nanotechnol. **5**, 722 (2010).
[57] L. Wang, I. Meric, P. Huang, Q. Gao, Y. Gao, H. Tran, T. Taniguchi, K. Watanabe, L. Campos, and D. Muller, Science **342**, 614 (2013).
[58] F. Pizzocchero, L. Gammelgaard, B. S. Jessen, J. M. Caridad, L. Wang, J. Hone, P. Bøggild, and T. J. Booth, Nat. Commun. **7**, 11894 (2016).
[59] L. Xie, L. Du, X. Lu, R. Yang, D. Shi, and G. Zhang, Chin. Phys. B **26**, 087306 (2017).
[60] J. Xue, J. Sanchez-Yamagishi, D. Bulmash, P. Jacquod, A. Deshpande, K. Watanabe, T. Taniguchi, P. Jarillo-Herrero, and B. J. LeRoy, Nat. Mater. **10**, 282 (2011).
[61] R. Ribeiro-Palau, C. Zhang, K. Watanabe, T. Taniguchi, J. Hone, and C. R. Dean, Science **361**, 690 (2018).
[62] A. Eckmann, J. Park, H. Yang, D. Elias, A. S. Mayorov, G. Yu, R. Jalil, K. S. Novoselov, R. V. Gorbachev, and M. Lazzeri, Nano Lett. **13**, 5242 (2013).
[63] B. Cheng, P. Wang, C. Pan, T. Miao, Y. Wu, T. Taniguchi, K. Watanabe, C. Lau, and M. Bockrath, Appl. Phys. Lett. **107**, 033101 (2015).
[64] D. Wang, G. Chen, C. Li, M. Cheng, W. Yang, S. Wu, G. Xie, J. Zhang, J. Zhao, X. Lu, P. Chen, G. Wang, J. Meng, J. Tang, R. Yang, C. He, D. Liu, D. Shi, K. Watanabe, T. Taniguchi *et al.*, Phys. Rev. Lett. **116**, 126101 (2016).
[65] N. R. Finney, M. Yankowitz, L. Muraleetharan, K. Watanabe, T. Taniguchi, C. R. Dean, and J. Hone, Nat. Nanotechnol. **14**, 1029 (2019).
[66] L. Ju, J. Velasco, Jr., E. Huang, S. Kahn, C. Nosiglia, H.-Z. Tsai, W. Yang, T. Taniguchi, K. Watanabe, and Y. Zhang, Nat. Nanotechnol. **9**, 348 (2014).
[67] A. Shukla, M. Calandra, M. d'Astuto, M. Lazzeri, F. Mauri, C. Bellin, M. Krisch, J. Karpinski, S. M. Kazakov, J. Jun, D. Daghero, and K. Parlinski, Phys. Rev. Lett. **90**, 095506 (2003).